Nano Energy 141 (2025) 111088

Contents lists available at ScienceDirect

Nano Energy

journal homepage: www.elsevier.com/locate/nanoen

Full paper

The triboelectric performance of natural friction materials from traditional Chinese herbs repository

Huirun Fan [a,c,e,1,2], Puchuan Tan [c,*,1,2], Yuan Bai [c], Yuan Xi [c,f], Engui Wang [c], Ming Yin [c], Xiaozhou Wen [c], Teng Li [a,e], Jiangtao Xue [c,g], Yang Zou [c,g], Zhou Li [b,c,d,**,3], Yang Wang [a,e,***,4]

[a] Institute of Integrative Medicine, Department of Integrated Traditional Chinese and Western Medicine, Xiangya Hospital, Central South University, Changsha 410008, China

[b] Tsinghua Changgung Hospital, School of Clinical Medicine, School of Biomedical Engineering, Tsinghua University, Beijing 100084, China

[c] Beijing Institute of Nanoenergy and Nanosystems, Chinese Academy of Sciences, Beijing 101400, China

[d] School of Nanoscience and Engineering, University of Chinese Academy of Sciences, Beijing 100049, China

[e] National Clinical Research Center for Geriatric Disorders, Xiangya Hospital, Central South University, Changsha 410008, China

[f] Beijing Advanced Innovation Centre for Biomedical Engineering, Key Laboratory for Biomechanics and Mechanobiology of Ministry of Education, School of Biological Science and Medical Engineering, School of Engineering Medicine, Beihang University, Beijing 100191, China

[g] School of Medical Technology, Beijing Institute of Technology, Beijing 100081, China

ARTICLE INFO

Keywords:
Traditional Chinese herbs
Triboelectric nanogenerator
Green energy

ABSTRACT

Triboelectric nanogenerator (TENG) is a highly efficient and environmentally friendly energy harvesting technology that has been widely used as a green self-powered energy supply device. However, the majority of current triboelectric materials rely on non-degradable polymers, which pose environmental issues. Natural materials offer advantages such as low cost and environmental friendliness, making them ideal candidates for the fabrication of green TENG. Considering the underutilization and significant waste of traditional Chinese herbs (TCH) resources, we design a traditional Chinese herbs-based triboelectric nanogenerator (TCH-TENG) and systematically investigates the triboelectric series of 20 kinds of TCHs. Among them, cinnabar exhibited the highest triboelectric performance, with an peak open-circuit Voltage (Voc) reaching 4.4 V and a peak short-circuit current (Isc) of 399 nA. TCH-TENG serves as a power source, successfully driving a set of commercial lights arrays and also achieving electrical stimulation of mice to induce gastrocnemius muscle contraction. This study combines the natural properties of herbs with TENG technology to propose a low-cost energy harvesting system, offering a novel solution for self-powered technologies in green energy.

1. Introduction

The excessive exploitation of fossil fuels has led to global environmental pollution[1] and climate change, accelerating the promotion and application of green and renewable energy. In this context, the sustainable use of natural resources and the development of environmentally friendly technologies have become important research directions globally. TENG has been widely used in the research of clean energy due to its advantages such as material diversity, high output, and high conversion efficiency[2,3]. At the same time, to promote the green

* Corresponding author.
** Corresponding author at: Tsinghua Changgung Hospital, School of Clinical Medicine, School of Biomedical Engineering, Tsinghua University, Beijing 100084, China.
*** Corresponding author at: Institute of Integrative Medicine, Department of Integrated Traditional Chinese and Western Medicine, Xiangya Hospital, Central South University, Changsha 410008, China.
E-mail addresses: tanpuchuan@binn.cas.cn (P. Tan), zli@binn.cas.cn (Z. Li), wangyang_xy87@csu.edu.cn (Y. Wang).
[1] co-first authors
[2] Huirun Fan and Puchuan Tan contributed equally to this work.
[3] ORCID: https://orcid.org/0000-0002-9952-7296
[4] ORCID: https://faculty.csu.edu.cn/wangyang1/zh_CN/index.htm

https://doi.org/10.1016/j.nanoen.2025.111088
Received 30 March 2025; Received in revised form 21 April 2025; Accepted 27 April 2025
Available online 29 April 2025
2211-2855/

development and quality improvement of the entire TCH industry chain, some TCHs have been used as energy materials to promote their efficient utilization[4–6]. To accelerate the industrialization of low-carbon green energy, the innovative integration of natural medicinal materials with TENG technology can achieve green and eco-friendly energy harvesting, providing new solutions for environmental protection and energy transformation[7].

Natural materials show great application potential for TENG due to their rich structural features and natural renewable properties[7–13]. For example, the team led by Andrei L. Kholkin at the University of Aveiro demonstrated that a TENG device based on dry leaves and polyvinylidene fluoride (PVDF)[14,15] successfully achieved a power output of up to 14 mW[11]. The natural structure and cellulose components of plant materials can significantly enhance the triboelectric effect, thereby improving energy harvesting efficiency. Some studies have also shown that natural materials can achieve more stable charge accumulation during triboelectrical, thereby increasing voltage and current output[16–20]. Through in-depth research on natural materials, scientists have made significant progress in energy harvesting technologies and have advanced green and environmentally friendly technologies[21–29].

In conclusion, this study has demonstrated the feasibility of using TCHs as triboelectric materials through comprehensive electrical characterization, and for the first time successfully established the triboelectric series of medicinal plants. The research confirms the potential of TCH-TENGs as green power supply systems, positioning herbal resources as breakthrough candidates for next-generation sustainable energy materials. These findings provide novel insights for sustainable energy development in the power sector, while simultaneously achieving resource recycling and value-added utilization in the field of TCHs.

2. Results and discussion

As shown in Fig. 1a, the schematic diagram of the TCH-TENG structure is presented. From top to bottom, the layers are as follows: Polydimethylsiloxane(PDMS) encapsulation layer, copper conductive layer, Polytetrafluoroethylene(PTFE) triboelectric layer, Chinese herb triboelectric layer, copper conductive layer, and PDMS encapsulation layer. PDMS was selected as the substrate material due to its low cost, good tensile strength, light weight, and ease of processing. The PDMS layers at both the top and bottom serve as substrates to ensure that the TCH-TENG does not deform easily. Copper tape is applied to the PDMS substrate as the conductive layer, with a copper wire attached to the bottom as the conductor. The processed TCH slices and PTFE are utilized as the triboelectric layers in the contact-separation TENG. Fig. 1b indicated the actual object image of the Chinese herbs selected as triboelectric layers, which have not undergone further processing. From left to right, the herbs include tortoise shell, piper kadsura, cnidii fructus, corn husk, cinnabar, and oyster. Fig. 1c illustrates the final TCH-TENG device we have prepared. Fig. 1d provides a schematic of the preparation process for the TCH-TENG. Firstly, the TCH were washed with deionized water and then placed in a vacuum dryer for 2 hours to remove all moisture. Afterward, the TCH were sliced and subjected to pressure using a tablet press to prepare TCH triboelectric layers. Finally, all materials were encapsulated with supporting layers to form the

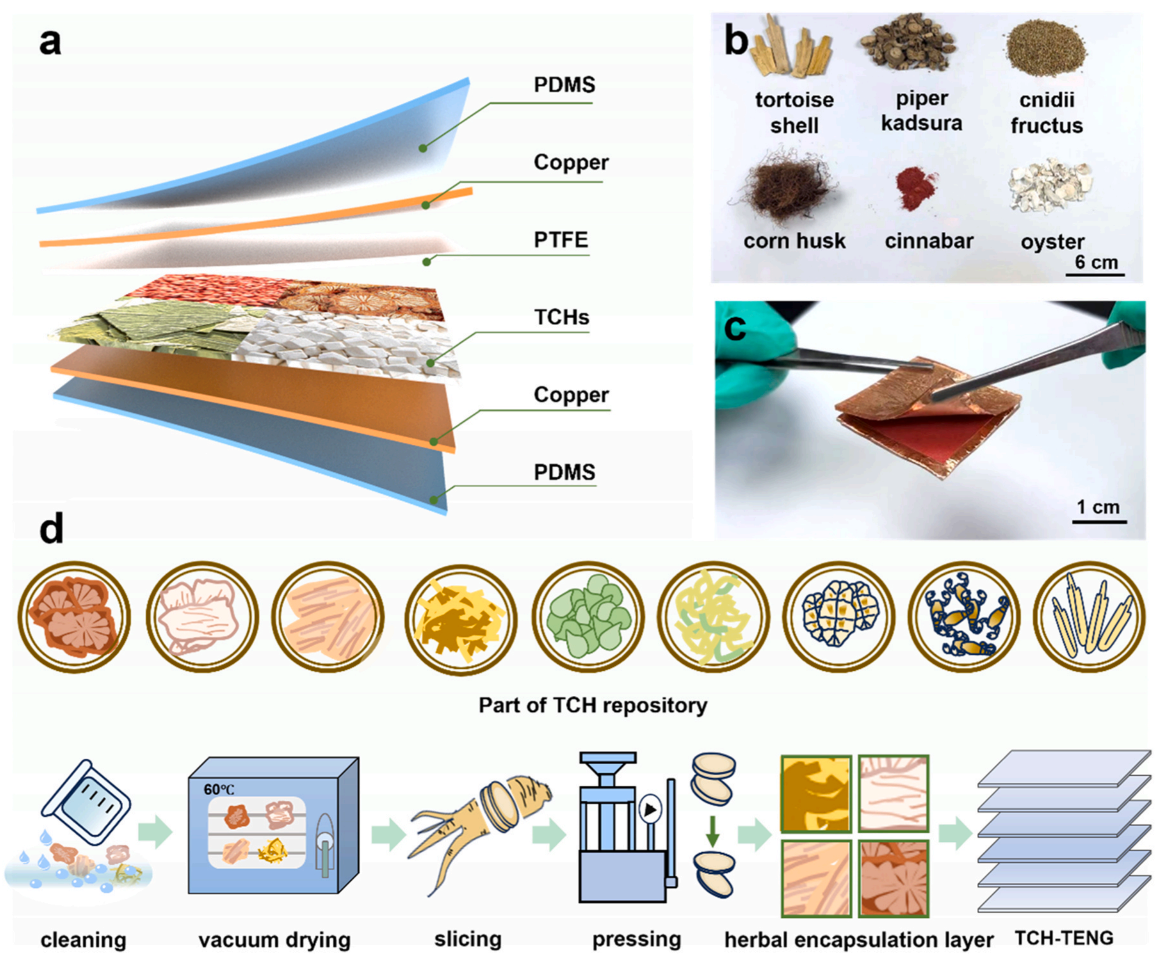

Fig. 1. The overview of TCH-TENG. (a) The structure of TCH-TENG. (b) Unprocessed Chinese herbal medicine samples. (c) Schematic diagram of TCH-TENG. (d) The preparation of TCH-TENG.

completed TCH-TENG.

In 2012, Wang et al.[30] developed a TENG that primarily converts mechanical energy into electrical energy by coupling the effects of electrostatic induction and triboelectric electrification[31]. TENG can be classified into four distinct working modes according to its motion form: contact-separation mode, single-electrode mode, sliding mode, and free electrode mode. This study employs the contact-separation mode teng. As shown in the Fig. 2a, under the action of an external force, the triboelectric layer of the TENG undergoes periodic contact and separation. One cycle of TENG motion can be divided into Four steps [32]: First, when two different materials (typically materials with differing electronegativities) come into contact, electrons transfer from one material to the other due to the triboelectric effect. This electron transfer results in an imbalance of charges on the surfaces of the two materials, resulting in the accumulation of different electrostatic charges on the surfaces of different triboelectrical layers. Then, when these materials separate, the difference in surface charges generates an electric field. This electric field drives the charges to flow through an external circuit, generating current. When the two materials reach their maximum separation, the current in the external circuit is zero, and the potential difference is at its maximum. Due to the different electrical properties of the materials, when they come into contact again, the charges are redistributed, returning the system to its initial state. This periodic process of contact and separation leads to the continuous

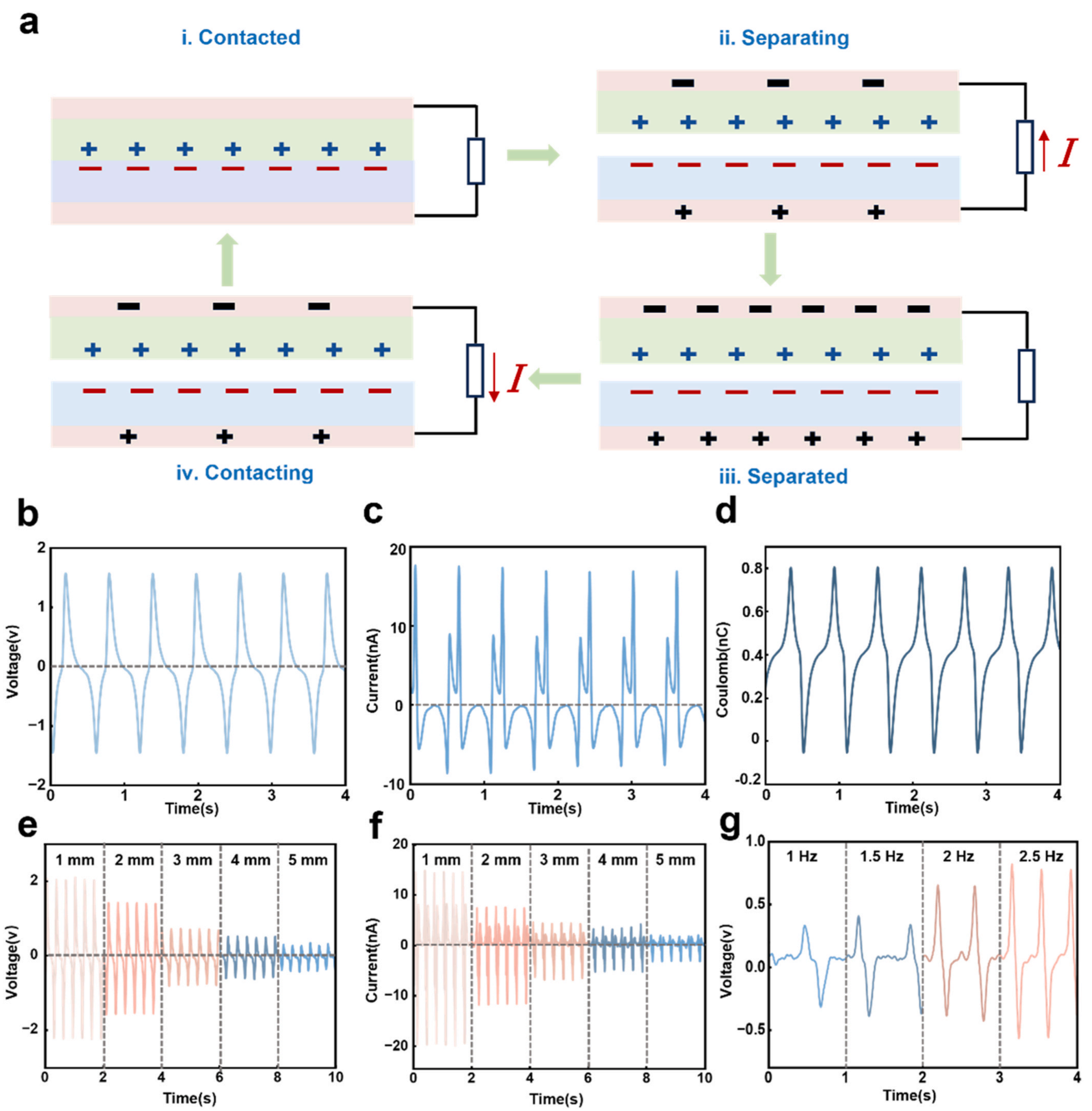

Fig. 2. Working principle of TCH-TENG and electrical testing and characterization. (a) Working principle of TCH-TENG. (b-d) Voltage, current output and charge transfer quantity of ginseng-TENG. (e-f) Voltage and current outputs of PTFE versus ginseng under different thickness. (g) Voltage and current outputs of PTFE versus ginseng under different frequency.

generation of alternating current. Due to the wide variety of TCH, before applying classification method based on medicinal parts, we first selected ginseng slices and PTFE as the triboelectric pair to fabricate the ginseng-TENG. We conduct electrical characterization tests on ginseng-TENG (The applied force was 20 N, with an area of 4 ×4 cm and a frequency of 1.5 Hz). As illustrated in the diagram Fig. 2b-d, the ginseng-TENG exhibited an peak Voc of 1.58 V, a peak Isc of 17.6 nA, and a charge transfer quantity of 1 nC. Due to the differences in thickness and frequency in actual energy collection environments[33], further research is needed to understand how the dielectric layer thickness and vibration frequency affect the output of the TENG device [34]. The equivalent capacitance model can be used to explain the impact of dielectric layer thickness on the output of the TENG[35,36]. The size of the capacitance determines how much charge can be stored, which in turn determines the surface charge density of the dielectric material. The thinner the dielectric material, the larger the equivalent capacitance, and the more charge it can store[37]. Therefore, within a certain thickness range, as the dielectric material thickness decreases, the output of the TENG gradually increases. And then we test the effect of thickness on ginseng-TENG electrical output (The applied force was 20 N, with an area of 4 ×4 cm and a frequency of 3 Hz), as shown in Fig. 2e-f. When the thickness of the ginseng triboelectrical layer decreased from 5 mm to 1 mm, peak Voc increased from 0.3 V to 2.1 V, peak Isc increased from 1.5 nA to 14.8 nA. The results demonstrate that as the thickness of the triboelectrical layer decreases, both the voltage and current output increase. When the frequency is the same, the amount of charge transferred is generally the same. However, at higher frequencies, the time required for charge transfer is shorter, leading to a significant increase in the peak Voc and peak Isc. As shown in Fig. 2g, when the frequency increases from 1 Hz to 2.5 Hz, peak Voc increased from 0.3 V to 0.82 V. Since the performance of TENG is directly proportional to the charge density on the contact surface, increasing charge generation has always been a key strategy to improve output power.

In this study, we selected 20 different TCHs based on their medicinal parts (as shown in Fig. 3a): animal-based TCH: turtle shell, tortoise shell, scorpion ground beetle, leech, chicken's gizzard-membrane; stems-based TCH: piper kadsura, bamboo ru; flowers-based TCH: honeysuckle, plum blossom; barks-based TCH: areca peel; seeds-based TCH: cnidii fructus; other-based TCH: corn husk; roots-based TCH: rhubarb; fungi-TCH: tuckahoe with pine; conchs -based TCH: mother-of-pearl mineral-based TCH: cinnabar, ocher, plaster, oyster. Their therapeutic effects and clinical applications are shown in Table S1. The TCH-TENGs are fabricated by these 20 TCH materials. We selected PTFE, which has a stronger electronegativity, and paper, which has a stronger electropositivity, according to the triboelectric series[38,39]. The same area (3 ×3 cm) was used for the positive and negative electrodes of the TCH-TENG, and the voltage and current outputs were measured separately. To evaluate the output performance of TCH-TENG, a linear motor device was utilized to apply mechanical loading. (The applied force was 20 N, with a frequency of 2.5 Hz). In Fig. 3b-c and Figure S1-9, we compared the peak Voc and peak Isc generated by 20 different TCHs triboelectrical layers (each with dimensions of 3 ×3 cm) when paired with PTFE and paper (each also 3 ×3 cm). When PTFE was used as the triboelectrical layer, the voltage range was 0.72 – 3.56 V, and the current range was 3.0 – 280 nA. When paper was used as the triboelectrical layer, the voltage range was 0.029 – 0.570 V, and the current range was 4.9 – 106.8 nA. In subsequent performance tests of other TENG, we selected the six TCHs with the highest output performance (indicated within the green dashed circle), which are as follows: tortoise shell, piper kadsura, cnidii fructus, corn husk, cinnabar, and oyster. The surface texture and roughness of different kinds of TCH catagory, resulting in differences in their electro-affinity. And then we paired TCHs with paper and PTFE respectively as triboelectric pairs, and their rankings in the triboelectric series are illustrated in the Fig. 3e and table S2, and the calculation formula used is in Equation[40]:

$$V = -\frac{Q}{S\varepsilon_0}(d_0 + x(t)) + \frac{\sigma x(t)}{\varepsilon_0}$$

$$V_{oc} = \frac{\sigma x(t)}{\varepsilon_0}$$

Where V is voltage, Q is charge, S is contact area, σ is the charge density, d is the thickness of the friction layer, ε_0 is the friction coefficient, and x is the spacing of the friction layer.

By analyzing the electrical output of the above 20 kinds of TCH-TENGs, we selected six TCHs with relatively better electrical performance for further investigation. First, we characterized the morphology of the six selected TCHs. Fig. 4a illustrates SEM image of six kinds of TCHs. Figure 4a1 indicates oyster, with an irregular, uneven surface. Figure 4a2 shows corn husk, displaying relatively regular arrangements of ridge-like structures. As illustrated in Figure 4a3, tortoise shell displays an uneven surface with long cracks, but is relatively smoother compared to the other five kinds of TCHs. Figure 4a4 reveals the surface of piper kadsura, exhibiting a nanoporous structure. Figure 4a5 express cnidii fructus, with a spindle-shaped structure that tapers at both ends and bulges in the middle, with ridge-like structures arranged in a regular pattern on the surface. Figure 4a6 is cinnabar, with irregular granular protrusions on the surface. Expanding the contact surface area is a direct way to enhance the total charge generated[33]. Among the six TCHs, cinnabar exhibited the most prominent granular surface morphology. When prepared as a tribolayer, it formed the densest structure with the largest effective contact area against PTFE, consequently demonstrating the highest electrical output. Oyster and cnidii fructus showed relatively sparse surface protrusions, yielding slightly lower performance than cinnabar. Piper kadsura and tortoise shell possessed moderately textured yet comparatively flatter surfaces, resulting in further reduced outputs. Due to its soft material properties, corn silk displays reduced contact-separation speed when interacting with the PTFE triboelectric layer, resulting in minimal power generation compared to other tested herbal materials. The effect of area on the electrical output of the TCH-TENG is revealed in Fig. 4b. The results indicate that the voltage and current output of the TCH-TENG have a linear relationship with the area. Take corn husk fructus as an example, the voltage and current also increase. When the area of PTFE/corn husk increased from 2 × 2 cm to 4 × 4 cm, peak Voc increased from 0.3 V to 0.78 V, peak Isc increased from 14.2 nA to 37.1 nA. The other five TCH-TENGs also generally follow the pattern where the output performance significantly improves as the area increases. As illustrated in Fig. 4c, we compared the electrical properties and current of six certain TCHs (The applied force was 20 N, with a frequency of 5 Hz and dimensions of 2.5 ×2.5 cm). Compared with paper, PTFE as a triboelectrical material produces higher peak Voc and peak Isc. When using PTFE as triboelectrical materiual, among the six certain TCHs, cinnabar exhibited the highest peak Voc and peak Isc, at 4.4 V and 399 nA, respectively. For tortoise shell, it showed the lowest peak Voc and peak Isc, at 0.88 V and 217 nA, respectively. The output of kadsura and corn husk were close to each other. When using paper as triboelectrical material, among the six certain TCHs, the peak Voc of cinnabar was 0.54 V, and the peak Isc was 53 nA, which are still the highest values. trtoiseshell had a peak Voc of 0.046 V and a peak Isc of 6.54 nA which represents lowest values.

The charging performance of TCH-TENG varies with different capacitance values. As shown in Fig. 5a, When charging a 1 μF capacitor with TCH-TENG, the voltage reaches 7.6 V within 30 s, and the charging process is completed in approximately 2.1 s. When charging a 3.3 μF capacitor with TCH-TENG, the voltage reaches 7.1 V within 30 s, and it reaches full charge in 12 s. When charging 10 μF, 33 μF, and 100 μF capacitors with TCH-TENG, the voltages reach 6.8 V, 4.8 V, and 2.2 V, respectively. Within 30 s, full charge is not achieved. This indicates that larger capacitors have relatively lower charging efficiency and require more time to accumulate charge.Long-term output stability is important

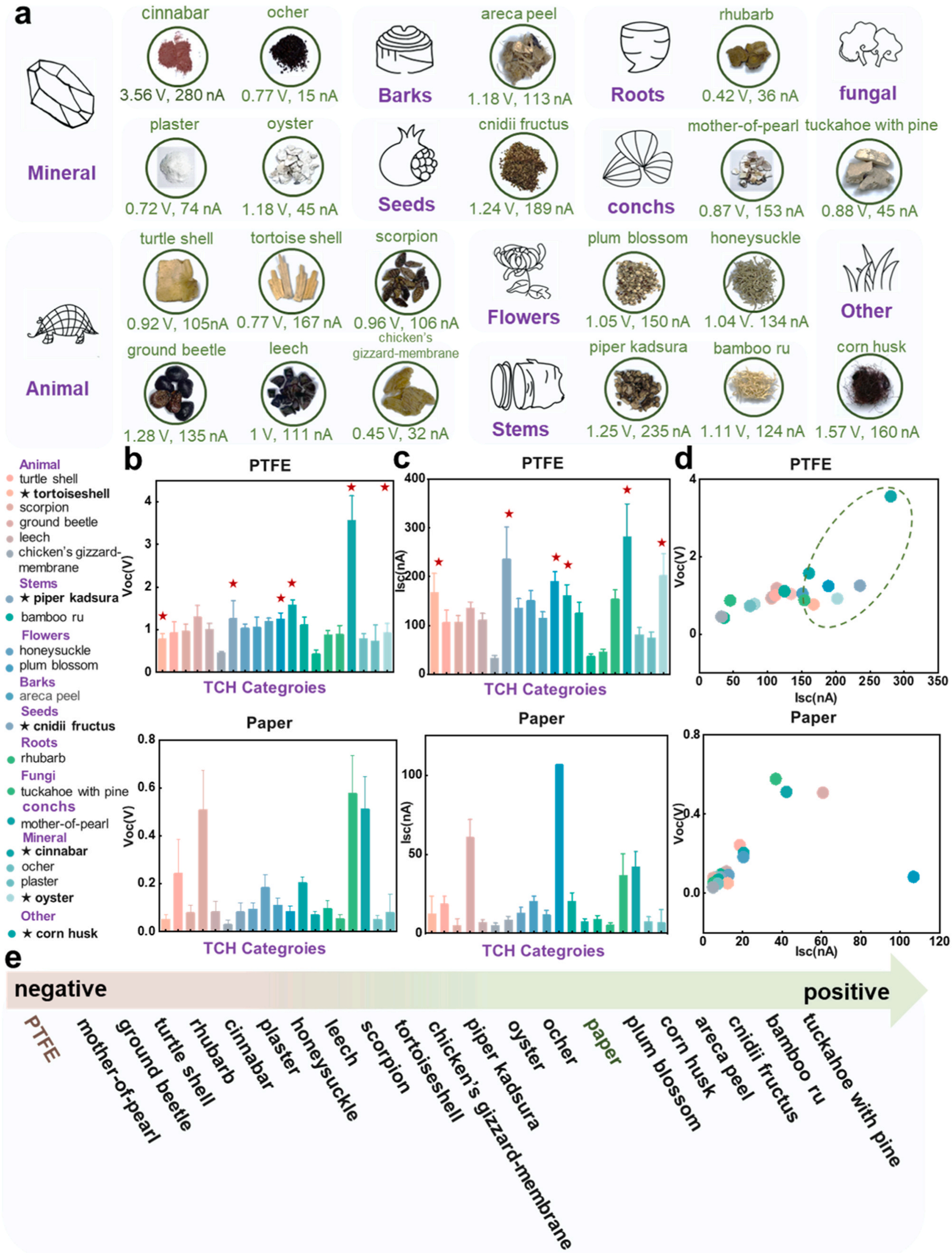

Fig. 3. The selected 20 kinds of TCHs are displayed along with their electrical performance. (a) The TCHs used in TCH-TENGs (classification method based on medicinal parts). (b-c) Comparison of peak Voc and peak Isc of different TCHs as triboelectrical layer and PTFE / paper as triboelectrical layer. (d) Ranking of 20 kinds of TCHs in the triboelectric series.

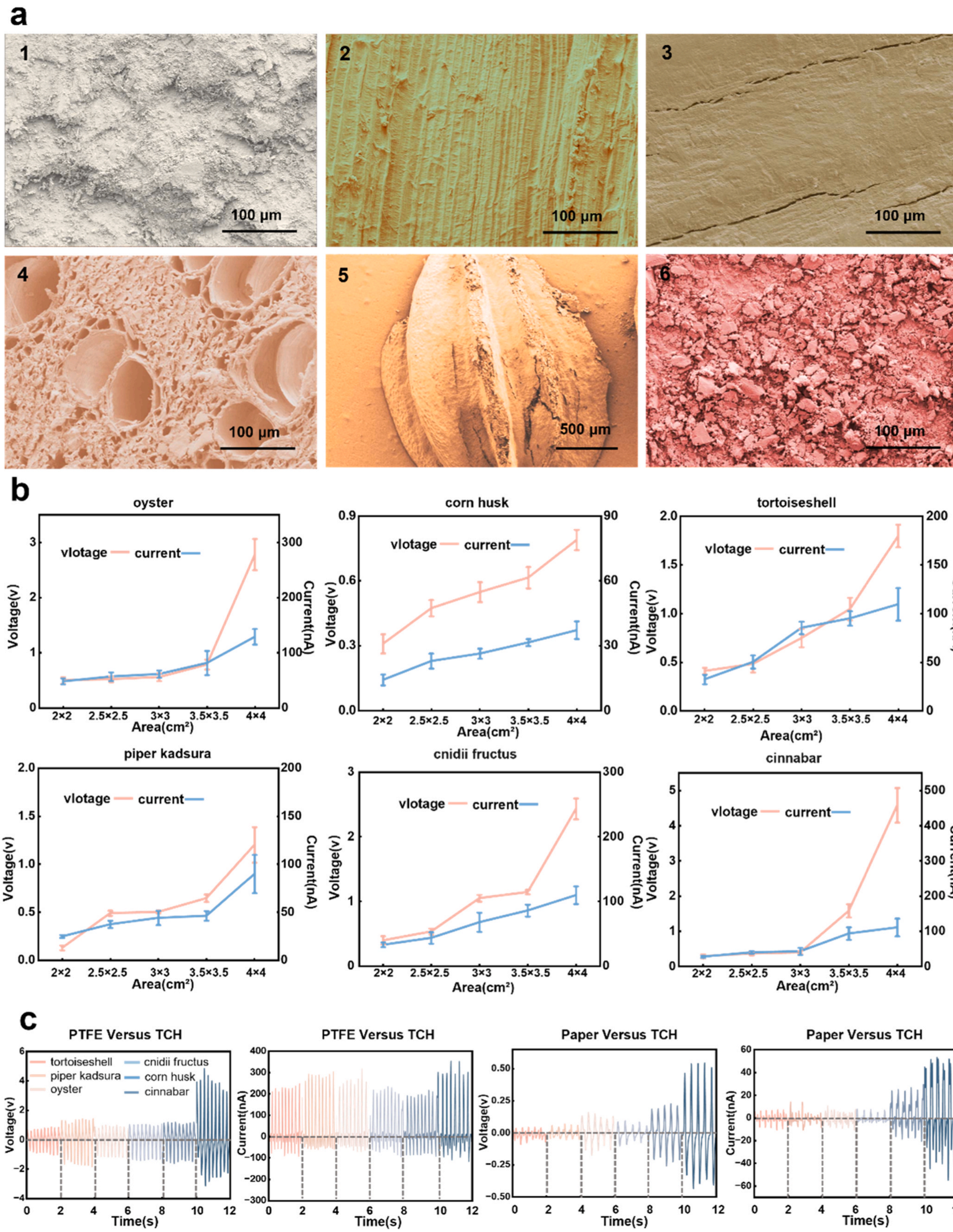

Fig. 4. SEM image of and electrical output pefermance of six certain TCHs. (a) SEM image of oyster, corn husk, tortoise shell, piper kadsura, cnidii fructus, cinnabar. (b) Voltage and current output of six certain TCHs as triboelectrical material in different area conditions.

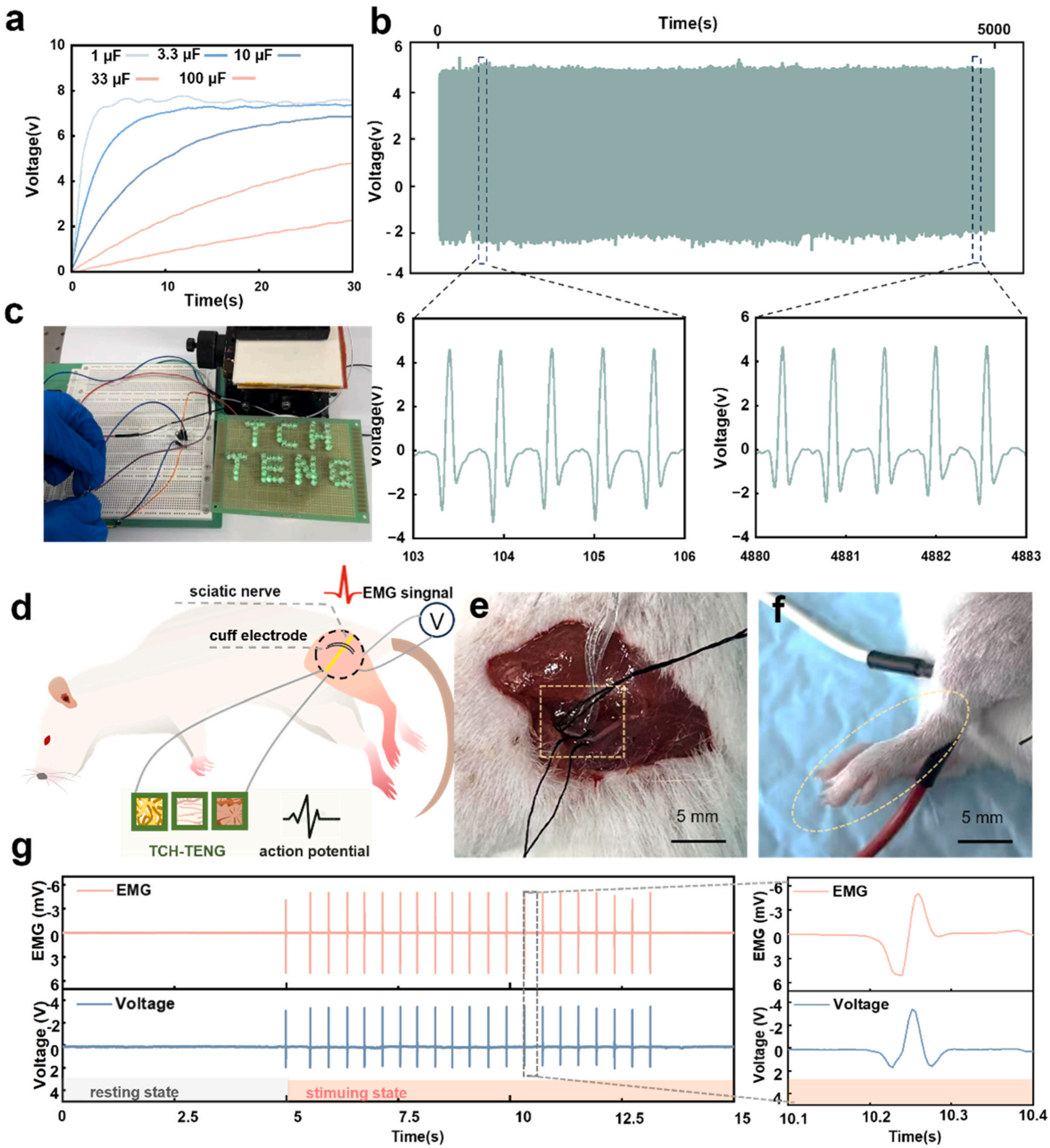

Fig. 5. Charging and discharging experiments of TCH and its potential applications (a) Charging different capacitors by the TCH-TENG. (b) Long-term working stability of TCH-TENG at 2 Hz for 10000 cycles. (c) The green LEDs are lit by TCH-TENG. (d) Peripheral nerve stimulation experiment conducted using TCH-TENG. (e-f) Stimulation of the sciatic nerve using a cuff electrode, resulting in contraction of the gastrocnemius muscle. (g) TCH-TENG voltage and EMG signal readings during sciatic nerve stimulation using a cuff electrode.

characteristic for assessing the practical application of TENG. As illustrated in Fig. 5b, after 10,000 cycles of continuous loading at a frequency of 2.5 Hz, the voltage output remains consistent with no significant attenuation, indicating excellent stability and durability for long-term use. Furthermore, as shown in Fig. 5c, due to the superior electrical output of TCH-TENG, the LED green light can be lit without the need for external storage devices. We utilized the TCH-TENG as a self-powered system to stimulate peripheral nerves, demonstrating the potential of traditional Chinese medicinal materials as power-generating sources for neural modulation. As shown in Fig. 5d, the cuff electrode was gently wrapped around the sciatic nerve of a rodent (highlighted by the yellow box in Fig. 5e), while a pair of needle electrodes were inserted into the gastrocnemius muscle to simultaneously record electromyography (EMG) signals. The TCH-TENG served as the power supply system, and an electrometer was used to measure the real-time voltage (Video S1). When the TCH-TENG underwent continuous contact-separation motion, we observed clear hindlimb twitching (highlighted by the yellow circle in Fig. 5f and Video S2). This occurs because the electrical stimulation generates action potentials in the sciatic nerve, which propagate along the nerve fibers as localized currents, ultimately inducing contraction of the gastrocnemius muscle. As shown in the Fig. 5g, the TCH-TENG generated an peak Voc of 3.4 V with an EMG signal peak of about 4.9 mV.

3. Conclusions

In Conclusion, TCH as natural plant, animal, and mineral materials, offer a rich variety of natural surface characteristics. Some of these materials possess complex microstructures on their surfaces, such as porous and ridge-like structures. These unique features not only expand the contact surface area but also significantly enhance the charge generation efficiency of the triboelectric electrodes. By compression molding, these medicinal materials were used to construct TCH-TENGs for energy harvesting and green energy conversion. This study systematically evaluated the output performance and durability of TCH-TENGs under different conditions. Experimental results show that under optimized conditions, the device achieves a maximum Voc of 4.4 V and Isc of 399 nA. After approximately 10,000 cycles of cyclic testing, the TCH-TENG maintains stable output, demonstrating excellent durability. These results confirm the substantial potential of medicinal materials as triboelectric electrode materials. Moreover, the electrical energy generated by the TCH-TENG is sufficient to power commercial LED lights and could also serve as a power supply system for bioelectrical stimulation, demonstrating its significant potential in green environmental energy harvesting and biological functionalities.

TCHs represent an eco-friendly and cost-effective class of natural materials for TENG fabrication. This study successfully developed TCH-TENGs, achieving sustainable valorization of medicinal resources while mitigating environmental risks associated with conventional energy technologies.

4. Experimental section

4.1. Fabrication of TCH-TENG

The dry TCHs were purchased the Tong Ren Tang pharmacy (Beijing, China). Then the dry medicinal materials are placed in molds of different sizes (4×4 cm, 3.5×3.5 cm, 3×3 cm, 2.5×2.5 cm, 2×2 cm), with the exposed parts serving as the contact area in the experiment. These exposed areas are attached to PDMS with the same surface area, and the metal electrodes are connected to the medicinal materials. A PTFE with the corresponding surface area is selected as the contact layer.

4.2. Characterization and measurement

The surface morphology of the TCHs was observed using SEM (SU8020, HITACHI, Japan). During the electrical output measurement, a commercial linear mechanical motor was used to apply external force. The oscilloscope (LeCroy, HDO6104, New York, USA) and Nanogenerator Analyzer (T5000–18A, Beijing, China) were used to measure and store data from the TCH-TENG. The electrometer (Keithley 6517) was used to measure the current and charge of the TCH-TENG.

4.3. Peripheral nerve modulation experiments in Kunming mouse model

The described peripheral nerve stimulation procedure was conducted in accordance with the approved animal use protocol 2025008LZ from the Beijing Institute of Nanoenergy and Nanosystems. Kunming mice (male, weights 30 g, ages 6 ~ 8 weeks) was anesthetized via intraperitoneal injection of 0.3 % sodium pentobarbital. A small incision was made to expose the sciatic nerve, and the incision was further enlarged to visualize the sciatic nerve. A cuff electrode was gently wrapped around the sciatic nerve, and a pair of stainless steel stimulating needle electrodes were inserted into the gastrocnemius muscle, spaced approximately 5 mm apart. EMG signals were recorded using a physiological signal acquisition system MP150. The TCH-TENG was then connected to the cuff electrode, and a vertical contact-separation force was applied to generate power. Simultaneously, the TCH-TENG was connected to an electrometer to record real-time voltage signals.

CRediT authorship contribution statement

Wang Engui: Visualization, Validation, Supervision. **Xi Yuan:** Visualization, Validation, Supervision. **Bai Yuan:** Visualization, Validation, Supervision. **Tan Puchuan:** Writing – review & editing, Visualization, Validation, Supervision, Methodology, Investigation, Funding acquisition, Formal analysis, Data curation, Conceptualization. **Wang Yang:** Writing – review & editing, Resources, Project administration, Methodology, Investigation, Funding acquisition, Conceptualization. **Fan Huirun:** Writing – review & editing, Writing – original draft, Visualization, Validation, Methodology, Investigation, Formal analysis, Data curation, Conceptualization. **Li Zhou:** Writing – review & editing, Resources, Project administration, Methodology, Investigation, Funding acquisition, Conceptualization. **Zou Yang:** Visualization, Validation, Supervision, Methodology. **Xue Jiangtao:** Visualization, Validation, Supervision. **Li Teng:** Validation, Supervision, Conceptualization. **Wen Xiaozhou:** Visualization, Validation, Supervision. **Yin Ming:** Visualization, Validation, Supervision.

Declaration of Competing Interest

The authors declare that they have no known competing financial interests or personal relationships that could have appeared to inffuence the work reported in this paper.

Acknowledgments

This study was supported by National Key R&D project from Minister of Science and Technology (2022YFB3804700), the National Natural Science Foundation of China (82274371). National Science Foudation of China (2023JJ30944), the National Natural Science Foundation of China (T2125003), China Postdoctoral Science Foundation (2023M743446), Beijing Natural Science Foundation (grant no. L245015) and the Fundamental Research Funds for the Central Universities. The authors are grateful to all the laboratory members for their cooperation in this study.

The table of contents entry

We prepared a green, eco-friendly, and low-cost TCH-TENG using traditional Chinese herbs, which can be used for energy harvesting and energy conversion.

Appendix A. Supporting information

Supplementary data associated with this article can be found in the online version at doi:10.1016/j.nanoen.2025.111088.

Data availability

Data will be made available on request.

References

[1] B.-Y. Chen, J.-H. Liao, C.-C. Hsueh, Z. Qu, A.-W. Hsu, C.-T. Chang, S. Zhang, Deciphering biostimulation strategy of using medicinal herbs and tea extracts for

bioelectricity generation in microbial fuel cells, Energy 161 (2018) 1042–1054, https://doi.org/10.1016/j.energy.2018.07.177.
[2] K. Tao, H. Yi, Y. Yang, H. Chang, J. Wu, L. Tang, Z. Yang, N. Wang, L. Hu, Y. Fu, J. Miao, W. Yuan, Origami-inspired electret-based triboelectric generator for biomechanical and ocean wave energy harvesting, Nano Energy 67 (2020), https://doi.org/10.1016/j.nanoen.2019.104197.
[3] D. Jiang, M. Du, X. Qu, Y. Gai, W. Sun, J. Xue, Y. Li, Z. Li, Z.L. Wang, Self-powered intelligent voice navigation tactile pavement based on high-output hybrid nanogenerator, Adv. Mater. Technol. 7 (2022), https://doi.org/10.1002/admt.202200270.
[4] H.-T. Deng, X.-R. Zhang, Z.-Y. Wang, D.-L. Wen, Y.-Y. Ba, B. Kim, M.-D. Han, H.-X. Zhang, X.-S. Zhang, Super-stretchable multi-sensing triboelectric nanogenerator based on liquid conductive composite, Nano Energy 83 (2021), https://doi.org/10.1016/j.nanoen.2021.105823.
[5] X. Cheng, B. Meng, X. Chen, M. Han, H. Chen, Z. Su, M. Shi, H. Zhang, Single-step fluorocarbon plasma treatment-induced wrinkle structure for high-performance triboelectric nanogenerator, Small 12 (2016) 229–236, https://doi.org/10.1002/smll.201502720.
[6] H. Wu, C. Shan, S. Fu, K. Li, J. Wang, S. Xu, G. Li, Q. Zhao, H. Guo, C. Hu, Efficient energy conversion mechanism and energy storage strategy for triboelectric nanogenerators, Nat. Commun. 15 (2024) 6558, https://doi.org/10.1038/s41467-024-50978-7.
[7] J. Liang, Y. Xu, C. Li, C. Yan, Z. Wang, J. Xu, L. Guo, Y. Li, Y. Zhang, H. Liu, H. Wang, Traditional Chinese medicine residue-derived micropore-rich porous carbon frameworks as efficient sulfur hosts for high-performance lithium-sulfur batteries, Dalton Trans. 51 (2021) 129–135, https://doi.org/10.1039/d1dt02595c.
[8] X. Li, Y. Chen, Y. Lai, Q. Yang, H. Hu, Y. Wang, Sustainable utilization of traditional Chinese medicine resources: systematic evaluation on different production modes, Evid. Based Complement Altern. Med 2015 (2015) 218901, https://doi.org/10.1155/2015/218901.
[9] E. Gering, D. Incorvaia, R. Henriksen, J. Conner, T. Getty, D. Wright, Getting back to nature: feralization in animals and plants, Trends Ecol. Evol. 34 (2019) 1137–1151, https://doi.org/10.1016/j.tree.2019.07.018.
[10] J. Gu, W. Zhang, H. Su, T. Fan, S. Zhu, Q. Liu, D. Zhang, Morphology genetic materials templated from natural species, Adv. Mater. 27 (2015) 464–478, https://doi.org/10.1002/adma.201401413.
[11] V. Slabov, S. Kopyl, M.P. Soares Dos Santos, A.L. Kholkin, Natural and eco-friendly materials for triboelectric energy harvesting, Nanomicro Lett. 12 (2020) 42, https://doi.org/10.1007/s40820-020-0373-y.
[12] K. Nanthagal, S. Khoonsap, V. Harnchana, P. Suphasorn, N. Chanlek, K. Sinthiptharakoon, K. Lapawae, S. Amnuaypanich, Unprecedented triboelectric effect of lignin on enhancing the electrical outputs of natural-rubber-based triboelectric nanogenerators (TENGs), ACS Sustain. Chem. Eng. 11 (2022) 1311–1323, https://doi.org/10.1021/acssuschemeng.2c03197.
[13] C. Yang, P. Xia, L. Zhao, R. Huang, K. Wang, H. Yang, Y. Yao, Hydrothermal carbonization of Chinese medicine residue from licorice: effects of pore and chemical structures on chromium migration, Ecotoxicol. Environ. Saf. 284 (2024) 116928, https://doi.org/10.1016/j.ecoenv.2024.116928.
[14] J. Pan, A. Jin, Improvement of output performance of the TENG Based on PVDF by doping tourmaline, ACS Sustain. Chem. Eng. 12 (2024) 2092–2099, https://doi.org/10.1021/acssuschemeng.3c07586.
[15] T. Huang, M. Lu, H. Yu, Q. Zhang, H. Wang, M. Zhu, Enhanced power output of a triboelectric nanogenerator composed of electrospun nanofiber mats doped with graphene oxide, Sci. Rep. 5 (2015) 13942, https://doi.org/10.1038/srep13942.
[16] D. Choi, D.W. Kim, D. Yoo, K.J. Cha, M. La, D.S. Kim, Spontaneous occurrence of liquid-solid contact electrification in nature: toward a robust triboelectric nanogenerator inspired by the natural lotus leaf, Nano Energy 36 (2017) 250–259, https://doi.org/10.1016/j.nanoen.2017.04.026.
[17] H. Wu, Z. Chen, G. Xu, J. Xu, Z. Wang, Y. Zi, Fully biodegradable water droplet energy harvester based on leaves of living plants, ACS Appl. Mater. Interfaces 12 (2020) 56060–56067, https://doi.org/10.1021/acsami.0c17601.
[18] R. Zhang, M. Hummelgård, J. Örtegren, M. Song, M. Olsen, H. Andersson, N. Blomquist, H. Olin, High performance single material-based triboelectric nanogenerators made of hetero-triboelectric half-cell plant skins, Nano Energy 94 (2022), https://doi.org/10.1016/j.nanoen.2022.106959.
[19] N.R. Alluri, N.P. Maria Joseph Raj, G. Khandelwal, V. Vivekananthan, S.-J. Kim, Aloe vera: A tropical desert plant to harness the mechanical energy by triboelectric and piezoelectric approaches, Nano Energy 73 (2020), https://doi.org/10.1016/j.nanoen.2020.104767.
[20] E.L. Tan, M.G. Potroz, G. Ferracci, J.A. Jackman, H. Jung, L. Wang, N.J. Cho, Light-induced surface modification of natural plant microparticles: toward colloidal science and cellular adhesion applications, Adv. Funct. Mater. 28 (2018), https://doi.org/10.1002/adfm.201707568.
[21] W. Jiang, H. Li, Z. Liu, Z. Li, J. Tian, B. Shi, Y. Zou, H. Ouyang, C. Zhao, L. Zhao, R. Sun, H. Zheng, Y. Fan, Z.L. Wang, Z. Li, Fully Bioabsorbable Natural-Materials-Based Triboelectric Nanogenerators, Adv. Mater. 30 (2018) e1801895, https://doi.org/10.1002/adma.201801895.
[22] R.A. Gross, B. Kalra, Biodegradable polymers for the environment, Science 297 (2002) 803–807, https://doi.org/10.1126/science.297.5582.803.
[23] S. Venkatraman, F. Boey, L.L. Lao, Implanted cardiovascular polymers: Natural, synthetic and bio-inspired, Prog. Polym. Sci. 33 (2008) 853–874, https://doi.org/10.1016/j.progpolymsci.2008.07.001.
[24] S. An, A. Sankaran, A.L. Yarin, Natural Biopolymer-Based Triboelectric Nanogenerators via Fast, Facile, Scalable Solution Blowing, ACS Appl. Mater. Interfaces 10 (2018) 37749–37759, https://doi.org/10.1021/acsami.8b15597.
[25] Z.L. Wang, Triboelectric nanogenerators as new energy technology for self-powered systems and as active mechanical and chemical sensors, ACS Nano 7 (2013) 9533–9557, https://doi.org/10.1021/nn404614z.
[26] C. Yao, A. Hernandez, Y. Yu, Z. Cai, X. Wang, Triboelectric nanogenerators and power-boards from cellulose nanofibrils and recycled materials, Nano Energy 30 (2016) 103–108, https://doi.org/10.1016/j.nanoen.2016.09.036.
[27] J. Meng, Q. Li, J. Huang, Z. Li, Tunable Schottky barrier height of a Pt-CuO junction via a triboelectric nanogenerator, Nanoscale 13 (2021) 17101–17105, https://doi.org/10.1039/d1nr04752c.
[28] S.L. Wei, W.Q. Wang, H. Wang, [Study on licorice resources and their sustainable utilization in center and western area of China], Zhongguo Zhong Yao Za Zhi 28 (2003) 202–206.
[29] G.V. Brigagão, O. de Queiroz Fernandes Araújo, J.L. de Medeiros, H. Mikulcic, N. Duic, A techno-economic analysis of thermochemical pathways for corncob-to-energy: Fast pyrolysis to bio-oil, gasification to methanol and combustion to electricity, Fuel Process. Technol. 193 (2019) 102–113, https://doi.org/10.1016/j.fuproc.2019.05.011.
[30] F.-R. Fan, Z.-Q. Tian, Z. Lin Wang, Flexible triboelectric generator, Nano Energy 1 (2012) 328–334, https://doi.org/10.1016/j.nanoen.2012.01.004.
[31] Y. Luo, X. Cao, Z.L. Wang, Self-powered smart agriculture sensing using triboelectric nanogenerators based on living plant leaves, Nano Energy 107 (2023), https://doi.org/10.1016/j.nanoen.2022.108097.
[32] H. Zhao, H. Wang, H. Yu, Q. Xu, X. Li, J. Guo, J. Shao, Z.L. Wang, M. Xu, W. Ding, Theoretical modeling of contact-separation mode triboelectric nanogenerators from initial charge distribution, Energy Environ. Sci. 17 (2024) 2228–2247, https://doi.org/10.1039/d3ee04143c.
[33] W.-Z. Song, T.-T. Zhang, D.-S. Zhang, C.-L. Li, D.-J. Sun, J. Zhang, S. Ramakrishna, Y.-Z. Long, Highly stretchable conductors reveal the effect of dielectric layer thickness on triboelectric nanogenerator output, Nano Energy 114 (2023), https://doi.org/10.1016/j.nanoen.2023.108621.
[34] B. Zhang, Y. Zou, M. Liu, E. Wang, X. Cui, Y. Wang, J. Xue, Y. Li, Y. Deng, Z. Li, Bacterial film-based degradable triboelectric nanogenerator for both contact and non-contact sensing, Chem. Eng. J. 500 (2024), https://doi.org/10.1016/j.cej.2024.156711.
[35] L. Long, W. Liu, Z. Wang, W. He, G. Li, Q. Tang, H. Guo, X. Pu, Y. Liu, C. Hu, High performance floating self-excited sliding triboelectric nanogenerator for micro mechanical energy harvesting, Nat. Commun. 12 (2021) 4689, https://doi.org/10.1038/s41467-021-25047-y.
[36] C. Li, Y. Bai, J. Shao, H. Meng, Z. Li, Strategies to Improve the Output Performance of Triboelectric Nanogenerators, Small Methods 8 (2024) e2301682, https://doi.org/10.1002/smtd.202301682.
[37] Y. Bai, S. Chen, H. Wang, E. Wang, X. Kong, Y. Gai, X. Qu, Q. Li, S. Xue, P. Guo, R. Wang, H. Feng, Z. Li, Chemical warfare agents decontamination via air mircoplasma excited by a triboelectric nanogenerator, Nano Energy 95 (2022), https://doi.org/10.1016/j.nanoen.2022.106992.
[38] H. Zou, Y. Zhang, L. Guo, P. Wang, X. He, G. Dai, H. Zheng, C. Chen, A.C. Wang, C. Xu, Z.L. Wang, Quantifying the triboelectric series, Nat. Commun. 10 (2019) 1427, https://doi.org/10.1038/s41467-019-09461-x.
[39] Z. Liu, S. Li, S. Lin, Y. Shi, P. Yang, X. Chen, Z.L. Wang, Crystallization-induced shift in a triboelectric series and even polarity reversal for elastic triboelectric materials, Nano Lett. 22 (2022) 4074–4082, https://doi.org/10.1021/acs.nanolett.2c00767.
[40] W. Zhong, L. long, N. Si, C. Jun, Z. Yu. Triboelectric Nanogenerator, 1st, ed, Science Press, Beijing, 2017.